Science of the Total Environment 654 (2019) 850–862

Contents lists available at ScienceDirect

Science of the Total Environment

journal homepage: www.elsevier.com/locate/scitotenv

Spatial distribution and temporal variation of drought in Inner Mongolia during 1901–2014 using Standardized Precipitation Evapotranspiration Index

Yongfang Wang [a], Guixiang Liu [a,*], Enliang Guo [b,c,d]

[a] Grassland Research Institute, Chinese Academy of Agricultural Sciences, Inner Mongolia, Hohhot 010010, PR China
[b] College of Geographical Science, Inner Mongolia Normal University, Hohhot 010022, PR China
[c] Inner Mongolia Key Laboratory of Disaster and Ecological Security on the Mongolian Plateau, Hohhot 010022, PR China
[d] Inner Mongolia Key Laboratory of Remote Sensing and Geographic Information Systems, Inner Mongolia Normal University, Hohhot 010022, PR China

HIGHLIGHTS

- SPEIbase v2.4 data was employed to extract SPEI in Inner Mongolia.
- BFAST is introduced to study the non-stationarity characteristics of drought.
- Central and eastern region of the study area showed a tendency towards drought.
- Intensity variation of drought showed an upturn, followed by a downtrend.
- Eastern and western regions exhibit opposite spatial gathering characteristics.

GRAPHICAL ABSTRACT

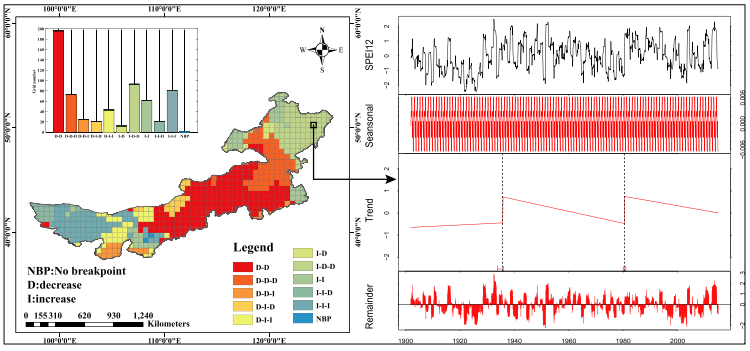

ARTICLE INFO

Article history:
Received 4 March 2018
Received in revised form 26 October 2018
Accepted 31 October 2018
Available online 3 November 2018

Editor: Damia Barcelo

Keywords:
Drought
BFAST
Non-stationarity
Intensity
Gathering characteristics

ABSTRACT

With intensification of climate change and human activities, warming and drying trend has brought severe challenges to pastoral areas in arid and semi-arid regions. Consequently, it becomes imperative to explore non-stationarity features of drought in such regions. In this research, the SPEIbase v2.4 datasets with a 0.5 degree spatial resolution was employed to extract Standardized Precipitation Evapotranspiration Index (SPEI) in Inner Mongolia, China. We explored non-stationarity characteristics of drought using Breaks For Additive Seasonal and Trend (BFAST) method, investigated the variation characteristics of drought intensity in each time interval using intensity analysis method, and finally assessed the spatial and temporal gathering characteristics of drought with Empirical Orthogonal Function (EOF). The results showed that trend of regional drought had a tendency towards drought conditions, which is particularly significant from the year 1945 onwards in the overall Inner Mongolia. We have explored a long behavior of drought in semiarid and central regions of cold semihumid climate zone throughout the whole study period, and detected a drying trend in northeastern regions of Inner Mongolia at the latter decades. The overall drought intensity displayed an increasing trend first, which was followed by a decreasing trend, among which the extreme drought was dominant in period of 1960–1970. EOF mode1 showed that variation intensity of drought showed a not significantly increasing trend in the entire region, and the drought with high amplitude was likely to occur in the central region. EOF mode2 showed that variation intensity of drought displayed the opposite phases between the eastern and the western regions. The northeastern regions were prone to display a high amplitude of drought.

* Corresponding author.
E-mail address: liuguixiang@caas.cn (G. Liu).

https://doi.org/10.1016/j.scitotenv.2018.10.425
0048-9697/

1. Introduction

Global warming is a major characteristic in the field of climate change, and a lot of research has been conducted by researchers and institutions around the world. For instance, the IPCC fifth assessment report pointed out that the global mean temperature increased by 0.85 °C from 1880 to 2012 (IPCC, 2014); The Global Risks Report 2017 released by World Economic Forum (WEF) classified climate change as the No.2 global risk. In the past one hundred years, the temperature has increased by 0.9–1.55 °C in land areas across China (NARCC, 2015); on August 11, 2016, Scientific Reports, an online multidisciplinary, open access journal from the publishers of Nature, pointed out that the number of flash droughts in China increased by 109% from 1979 to 2010, and global warming would increase the occurrence of flash drought in future decades across China (Wang et al., 2016a). Since the 1900s, human beings have witnessed most dramatic societal changes. Due to rapid social development, particularly since China's reform and opening-up policy in 1978, China has embarked on a course of rapid development, with an ever-increasing rate of urbanization. In China, climate change and human activities have been exerting unprecedented influence on the environment that humans are living in, which rapidly alter the structure and function of ecosystems. Among these phenomena, the droughts caused by abnormal climate system have occurred more and more frequently, which exerts a strong impact on ecosystems, human production and life (Wang et al., 2014). Consequently, the loss of drought has been on a constant rise by years (He et al., 2013; Huang et al., 2016).

Featured with little rainfall, low soil moisture, and shortage of water resources for agricultural and socio-economic activities, the droughts were generally classified into four types, which included meteorological drought, hydrological drought, agricultural drought, and socio-economic drought (Mishra and Singh, 2010). Among these, meteorological drought was a major inducing factor for the other three drought categories. It was studied on the basis of its frequency, duration, severity and spatial variation in terms of a region or using specific index. Consequently, many drought indices were derived accordingly, including Standardized Wetness Index (SWI) (Liu et al., 2017a), Palmer Drought Severity Index (PDSI) (Palmer, 1965; Liu et al., 2017b), Standardized Precipitation Index (SPI) (McKee et al., 1993), Composite Meteorological Drought Index (CI) (Guo et al., 2017), the Standardized Precipitation Evapotranspiration Index (SPEI) etc. (Vicenteserrano et al., 2010; Zhang et al., 2017; Wang et al., 2018). Generally, each drought index requires specific input parameters in order to measure drought (Mishra and Singh, 2010). For example, The SPI was calculated using long-term records of monthly precipitation with at least 30-year records (Wu et al., 2005), while precipitation and temperature was used to calculate the PDSI and SPEI. Sheffield and Wood (2008) considered that the variability of temperature had important effects on drought conditions, as it could dramatically change the land surface water balance by controlling evapotranspiration. The scholars also found that evapotranspiration consumed 80% of the precipitation. When the amount of evapotranspiration increased, the regional water demand would also increase, thus increasing the intensity and extent of the drought (Abramopoulos et al., 1988; Thornthwaite, 1948; Li et al., 2012). Further considering the impacts of meteorological variables on drought, the SPEI was applied in our study. It not only contained features of multiple time scales, the consideration of evapotranspiration in the water balance was the key point that allowed the SPEI to identify the influences of fluctuations and trends of temperature and evapotranspiration on drought conditions in the context of global warming (Liu et al., 2016a).

Inner Mongolia is a major production base for animal husbandry and pasture resources in China. In recent years, however, the intensification of climate change and human activities has led to ecological environment deterioration, grassland degeneration and desertification, in particular, which results in frequent occurrence of drought disasters, and directly undermines agriculture and animal husbandry on which farmers and herdsmen uplift their living standards. Therefore, the investigation on long-term development patterns of drought in Inner Mongolia could help improve the understanding of causes, risk management, and prevention of drought disasters in the region. Studies have been conducted in this region to analyze the spatiotemporal characteristics of droughts using different drought indices and mathematical statistics. Using Standardized Precipitation Evapotranspiration Index, Liu et al. (2016b) investigated the drought variability in Inner Mongolia of northern China during the period of 1960–2013. Huang et al. (2015) analyzed the spatial and temporal variability of drought in Inner Mongolia using standard precipitation index and dry spells from 1960 to 2012. Tong et al. (2018) investigated the variations and patterns of drought in the Mongolian Plateau for the period of 1980–2014 using the Standardized Precipitation Evapotranspiration Index. The previous studies always looking for a linear trend of drought, which erased the extreme events to a large extent, it was difficult to obtain the detail change characteristic of drought events. Moreover, traditional methods, such as Mann-Kendall (MK) mutation detection, Modified Mann-Kendall (MMK) mutation detection among others, have been often used to determine the breakpoints of drought variation. However, the methods limit the mining of drought variation information to a certain extent, and fail to effectively analyze how drought changes in different time intervals and clustering phenomena in time series. For SPEI, featured with multi-scale, multi-layer and non-stationarity, drought is a process that occurs slowly and increases gradually in intensity. Thus, Breaks For Additive Seasonal and Trend (BFAST), a method can simultaneously explore the non-stationarity trend characteristics and breakpoint of drought, was introduced in our study. BFAST has been widely used in the field of NDVI research in recent years, which could conduct trend analysis and seasonal change characteristics in time series, and detect periodical change patterns and determine its fluctuation, and effectively describe the changing pattern of the breakpoint time in particular (Verbesselt et al., 2010a). At the same time, intensity analysis method was also applied in our study to investigate the annual changes, changes among different drought categories, and the pattern of drought transitions. The method was proposed by Aldwaik Jr and Pontius (2012) to quantitatively analyze Land Use and Cover Change (LUCC). Using the transition of land uses within the same region and at the same time point, it employed a transition matrix to analyze patterns of variation intensity of land uses at three levels: the interval level, the category level, and the transition level. Similarly, transition occurs among different drought categories within different intervals in the same region. Thus, intensity analysis method can be introduced into drought research to address three questions: (1) is annual change of each drought category within the same interval relatively fast versus slow? (2) Is change of a drought category relatively dormant versus active? And (3) in the process of transition of drought category, which category dominates the transition process? Besides, in order to get deeper understanding of drought change after using BFAST and intensity analysis methods, we also introduced the Empirical Orthogonal Function (EOF) method to assess the spatial and temporal gathering of drought variation intensity, which could help explore spatial distribution and temporal variation of droughts with non-stationarity characteristics in Inner Mongolia.

Overall, the objective of this study was (1) to explore the temporal and spatial variation of non-stationarity characteristics of drought by using BFAST method; (2) to investigate the variation characteristics of intensities among drought categories in each decade during 1901–2014 by applying intensity analysis method; and (3) to assess the gathering characteristics of drought on spatiotemporal scale by adopting EOF method in Inner Mongolia.

2. Materials and methods

2.1. Materials

Inner Mongolia, located at the central region of Eurasian continent and northern border area of China, stretches 2400 km from west to

east. It is a provincial administrative region with the widest span of longitudes in China (from 97°12′E to 126°04′E in longitude and from 37°24′N to 53°23′N in latitude). The southeast wind in summer has varying degrees of influence on different areas in Inner Mongolia due to variation in their distance to the coast, which leads to a climate with high temperature and rainy weather, being rainy and hot during the same period. In winter, however, the region has a dry and cold weather due to the influence of Siberia-Mongolia high pressure (Fig. 1).

The gridded SPEI was derived from SPEIbase v2.4, based on monthly precipitation and potential evapotranspiration of the CRU TS 3.23 dataset from the Climatic Research Unit of the University of East Anglia. Such data were derived from the FAO-56 Penman-Monteith estimation of potential evapotranspiration. Therefore, the SPEIbase was recommended for long-term climatological analysis, which covered the period between January 1901 and December 2014. The data were featured with a multi-scale character, providing SPEI time-scales between 1 and 48 months with 0.5 degree spatial resolution (Vicenteserrano et al., 2010). In this study, we used administrative boundary of Inner Mongolia to extract the gridded SPET within the study and surrounding areas. 626 grids of SPEI were used in this study, and the drought severity was classified according to the SPEI grade standard (Wang et al., 2016b) (Table S1).

In order to evaluate the spatiotemporal performance capacity of drought using SPEIbase v2.4 in Inner Mongolia, we compared and analyzed the observed SPEI and the gridded SPEI. The observed SPEI was based on monthly precipitation and monthly average temperature of 46 weather stations during 1961–2014, which were downloaded from China Meteorological Data Service Center (http://data.cma.cn/site/index.html). The corresponding geographical coordinates of the meteorological stations were provided in the supplementary materials (Table S2). Inner Mongolia belongs to the arid, semiarid and cold semihumid climatic zones based on Köppen climate classifications, and climate change will exert a drastic impact on the entire region (Chen et al., 2017). SPEI at different scales has different levels of sensitivity towards climate change. Because the research period of the paper has exceeded 100 years, thus, SPEI12 was chosen. It can reveal the drought variation on an interannual scale as it is less sensitive to short-term precipitation and temperature, and the variation of drought characterized by SPEI12 will be more significant, meeting the needs of the paper.

In order to perform attribution analysis of climate change on drought evolution, we also used TerraClimate dataset from 1958 to 2014 to extract meteorological factors, including actual evapotranspiration (AET), climate water deficit (DEF), potential evapotranspiration (PET), soil moisture (SM), downward surface shortwave radiation (SRAD), max temperature (TMAX), min temperature (TMIN), wind speed (WS), which were created by using climatically aided interpolation, combining the WorldClim version 1.4 and version 2 datasets with CRU Ts4.0 and JRA-55 (Abatzoglou et al., 2018). To match the grid point, we also calculated mean values of a pixel within the zones of TerraClimate for 626 grid points in Inner Mongolia.

2.2. Methods

2.2.1. Breaks For Additive Seasonal and Trend (BFAST)

BFAST iteratively estimates the time and number of abrupt changes within time series, and characterizes change by its magnitude and

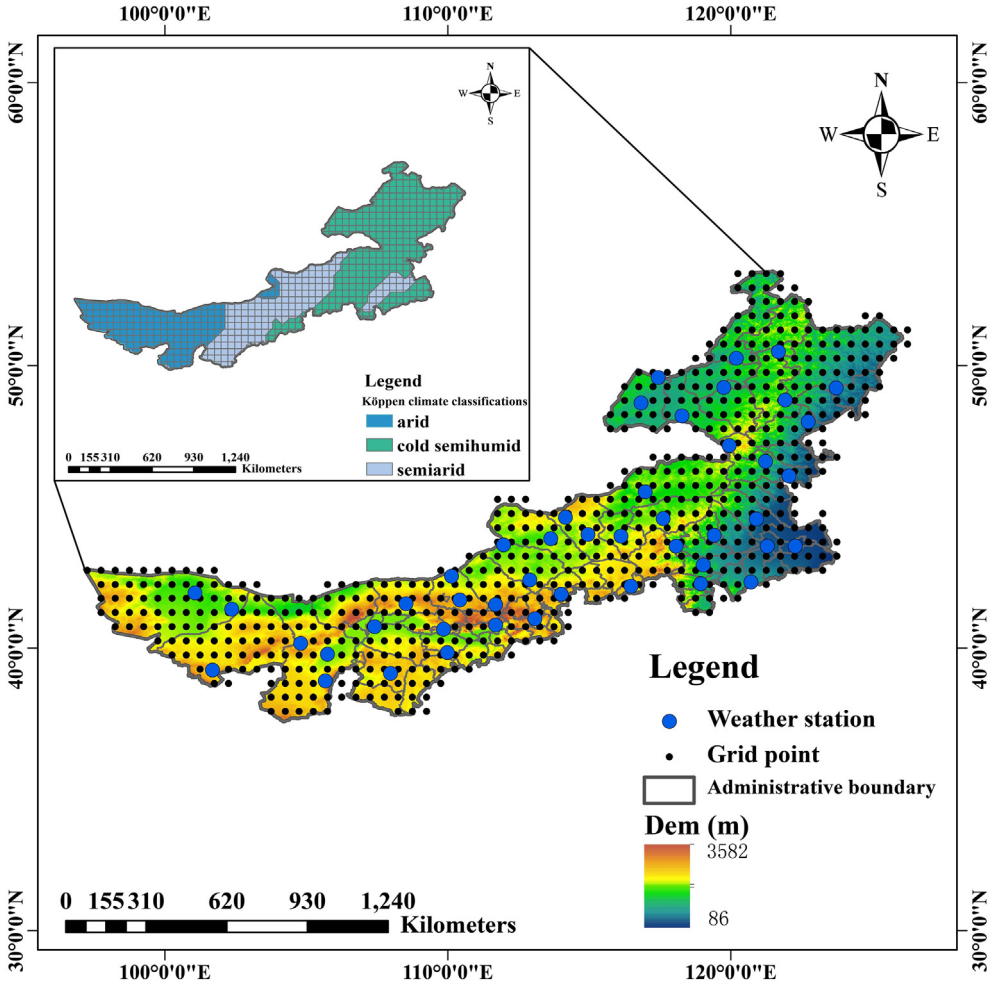

Fig. 1. The spatial distribution of climatic zones and stations in this study.

direction. BFAST can be used to analyze different types of time series and can be applied to other disciplines dealing with seasonal or non-seasonal time series, such as hydrology, climatology, and econometrics. BFAST was employed to iteratively fit a piecewise linear trend and a seasonal model (Verbesselt et al., 2010b). The general model is as follows:

$$Y_t = T_t + S_t + e_t, t = 1, \cdots n \tag{1}$$

where Y_t is the monthly gridded SPEI12 value of each grid during 1901–2014 in Inner Mongolia, T_t is the trend component (Trend), S_t is the seasonal component (Seasonal), and e_t is the remainder component (Remainder). The seasonal component can be used to monitor phenological variations of activity; the trend component can detect the abrupt and gradual change at a long time scale; and remainder component related to irregular short-term variations or noise (e.g., clouds or atmospheric scatter) (Lambert et al., 2015; Li et al., 2017). The main objective of the study is to explore whether there is a non-stationarity characteristic at a long time scale of drought, and if it exists, what is the breakpoint and change of trend before and after it? On the other hand, the use of SPEI12 to fit seasonal components is of little significance. Therefore, this paper focused on the application of the trend component in temporal and spatial variation of drought.

The long-term trend component, T_t, is piecewise linear with segment-specific slopes and intercepts on m + 1 different segments. Thus, there are m breakpoints $\tau_{i-1}, \cdots \tau_m$ so that

$$T_t = \alpha_i + \beta_i t \tag{2}$$

where $i = 1, 2, \cdots m$ and we define $\tau_0 = 0$ and $\tau_{m+1} = n$. The order of magnitude of breakpoints, M, can be calculated with the intercepts α_i and β_i of the linear model T_t between t_{i-1} and t_i as follows:

$$M = (\alpha_{i-1} - \alpha_i) + (\beta_{i-1} - \beta_i)t \tag{3}$$

In the long-term trend component, the number of breakpoints and their positions in the time series were determined using Least Square Method and Bayesian Information Criterion. Specifically, a moving average summation of Least Square Method was used to test and determine whether there were breakpoints, and Bayesian Information Criterion was used to determine the minimum number of breakpoints, and Least Square Method was employed to estimate the position of breakpoints in time series (Grogan et al., 2016; Tian et al., 2015; Verbesselt et al., 2012). BFAST employs minimal segment size, h, between potentially detected breaks in the trend model given as fraction relative to the sample size (i.e. the minimal number of observations in each segment divided by the total length of the time series). Suppose the span of time series is 10 years, when $h = 0.1$, the time interval of two breakpoints determined by minimal segment size should be 1 year, indicating that if there are two breakpoints within 1 year, only the more remarkable one can be detected.

2.2.2. Intensity analysis method

According to the calculation principle of intensity analysis method, the intensity of drought at different time interval needs to be classified into categories (Tong et al., 2018). In this paper, drought intensity at a time interval for each grid point was calculated as follows:

$$D_{ij} = \left| \frac{1}{m} \sum_{i=1}^{m} SPEI_i \right| \tag{5}$$

where m is the frequency of drought for each the grid. $SPEI_i$ is the absolute value of the corresponding SPEI when drought occurs (Zhou et al., 2013). It is a drought event if the SPEI value is less than −0.5. $D_{ij} < 0.5$ indicates that no drought has occurred; $1 > D_{ij} \geq 0.5$ indicates mild drought; $1.5 > D_{ij} \geq 1$ indicates moderate drought; $2 > D_{ij} \geq 1.5$ indicates severe drought; and $D_{ij} \geq 2$ indicates extreme drought. When droughts were classified into categories within the time interval, it met the input requirements for data format in intensity analysis method. At the same time, the information of drought intensity in each year was also integrated into time interval. We classified drought of each grid into categories, and counted the number of grids of transition from one-time interval to the next time interval for each drought category.

2.2.3. Empirical Orthogonal Function (EOF) analysis method

Empirical Orthogonal Function (EOF) analysis method is a widely used spatial decomposition method in the field of climate change (Dai et al., 2004). It presents the gridded SPEI index in the form of a matrix (m is the number of grids and n is the length of SPEI index series):

$$X_{m\times n} = \begin{pmatrix} x_{11} & x_{12} & \cdots & x_{1n} \\ x_{21} & x_{22} & \cdots & x_{2n} \\ \cdots & \cdots & \cdots & \cdots \\ x_{m1} & x_{m2} & \cdots & x_{mn} \end{pmatrix} \tag{6}$$

Variable $X_{m\times n}$ can be regarded as a linear combination of p spatial eigenvectors and their corresponding time weight coefficients:

$$X_{m\times n} = V_{m\times p} T_{p\times n} \tag{7}$$

where T is time coefficient of SPEI index, and V is spatial eigenvector of SPEI index. Thus, the main information of the variate field can be represented by several typical eigenvectors. To investigate time change patterns and spatial modes when drought occurred in Inner Mongolia, this paper conducted EOF decomposition towards annual average variate field of SPEI, extracted the spatial modes and their corresponding time coefficients, and revealed the temporal and spatial variation of droughts.

Significance test was conducted, since random numbers or false data could also produce spatial eigenvectors and principal components if they were decomposed in EOF analysis, whether spatial modes derived from real data analysis were random or not should be determined by statistical testing (North et al., 1982). The error of the eigenvalue at 95% confidence level can be verified by

$$\Delta\lambda = \lambda\sqrt{\frac{2}{N^*}} \tag{8}$$

where $\Delta\lambda$ is error of the eigenvalue; λ is eigenvalue of each modal; and N^* is effective degree of freedom. λ should be checked in sequence, and corresponding error range should be provided. If error ranges of two λ are overlap with each other, it fails to pass the significance test.

3. Results

3.1. Applicability analysis of SPEIbase v.2.4

In this paper, we used monthly precipitation and monthly average temperature data to calculate SPEI12 of 46 weather stations, and compared them with the gridded SPEI12, which covered the period between January 1961 and December 2014. A curve fit was performed on the regional average of observed SPEI12 and gridded SPEI12. The results showed that the two groups of data showed a significant linear correlation and their correction coefficient was 0.8306 (Fig. 2a), suggesting that the average value of the grid SPEI12 can be used to analyze the variation of regional drought at the temporal scale. In order to evaluate the spatial correlation between observed SPEI12 and gridded SPEI12, this paper also calculated Pearson correlation coefficients and Root Mean Squared Error (RMSE) for them. The results suggested that the spatial correlation between observed SPEI12 and gridded SPEI12 in the eastern region was larger than that in the western region (Fig. 2b and c). However, as for the spatial distribution of drought, the correlation coefficients between the observed SPEI and the gridded SPEI in all stations were above the 95% confidence level in Inner Mongolia. Thus, gridded

SPEI12 can be applied to analyze spatial variation of drought in the study area.

3.2. Exploration of non-stationarity characteristics of drought

3.2.1. Temporal variation of regional drought

The BFAST method was used to decompose the regional SPEI12 value, and it was found that there were breakpoints within long-term time series of SPEI12, which meant that the drought in the entire Inner Mongolia showed non-stationarity. The breakpoint occurred in 1945 (Fig. 3); the study area showed a tendency towards drought both before and after the breakpoint time. During the interval of 1901–1945, the amplitude of trend of regional SPEI12 was −0.00014/a and below the 95% confidence level while that of SPEI12 during the interval of 1946–2014 was −0.007/a, which was above the 95% confidence level, suggesting that the trend of drought became particularly apparent during this time interval. Overall, climate in Inner Mongolia became drier during 1901–2014, but the trend is even more pronounced after 1945.

3.2.2. Spatial variation of non-stationarity characteristics of drought

To explore the spatial variation of non-stationarity characteristics of drought in Inner Mongolia, we also introduced BFAST method to this section. Unlike the previous section, we used the BFAST algorithm to decompose the SPEI12 value for each grid, and then a spatial distribution of variation types of trend was obtained (Fig. 4). There were 11 variation types and significant spatial differences in SPEI12, only two grids of drought index were not breakpoints in the semiarid zone. There were 196 grids of decrease-decrease (D-D) variation type that were mainly distributed in central region, among which 110 grids belonged to the semiarid zone and 77 grids in the cold semiarid zone. 73 grids were the decrease-decrease-decrease (D-D-D) variation type that mainly concentrated in the central part of the cold semihumid zone. The area where the SPEI12 showed D-D and D-D-D type suggested that the climate in these areas was becoming increasingly dry in the past one hundred years. 142 grids of drought index continued to increase, among which 61 grids presented as the increase-increase (I-I) variation type, scattered in the northeastern and western regions of the study area, and the grids in the semiarid zone accounted for 73.8% of the total I-I type grids. The other 81 grids belonged to increase-increase-increase (I-I-I) variation type, which were mainly distributed in the western region.

Additionally, opposite trends were observed before and after breakpoints, among which 93 grids belonged to increase-decrease-decrease (I-D-D) type, accounting for the largest proportion, and they were mainly distributed in the northeastern region which belonged to the cold semihumid zone. It suggested that in these regions, the intensity of drought event might decrease first, and then continue to increase

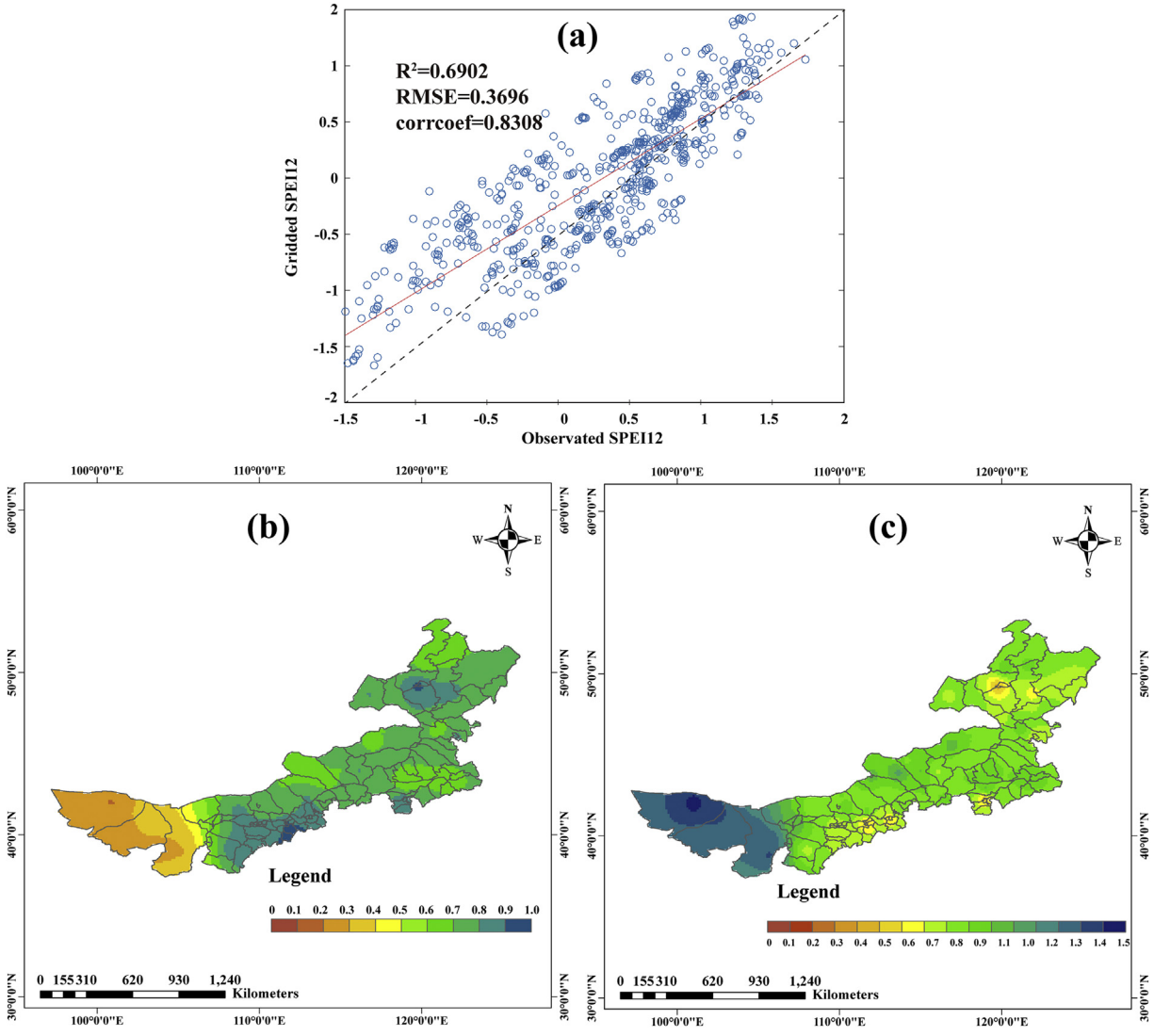

Fig. 2. Evaluation of the spatiotemporal performance of SPEIbase v.2.4 in Inner Mongolia.

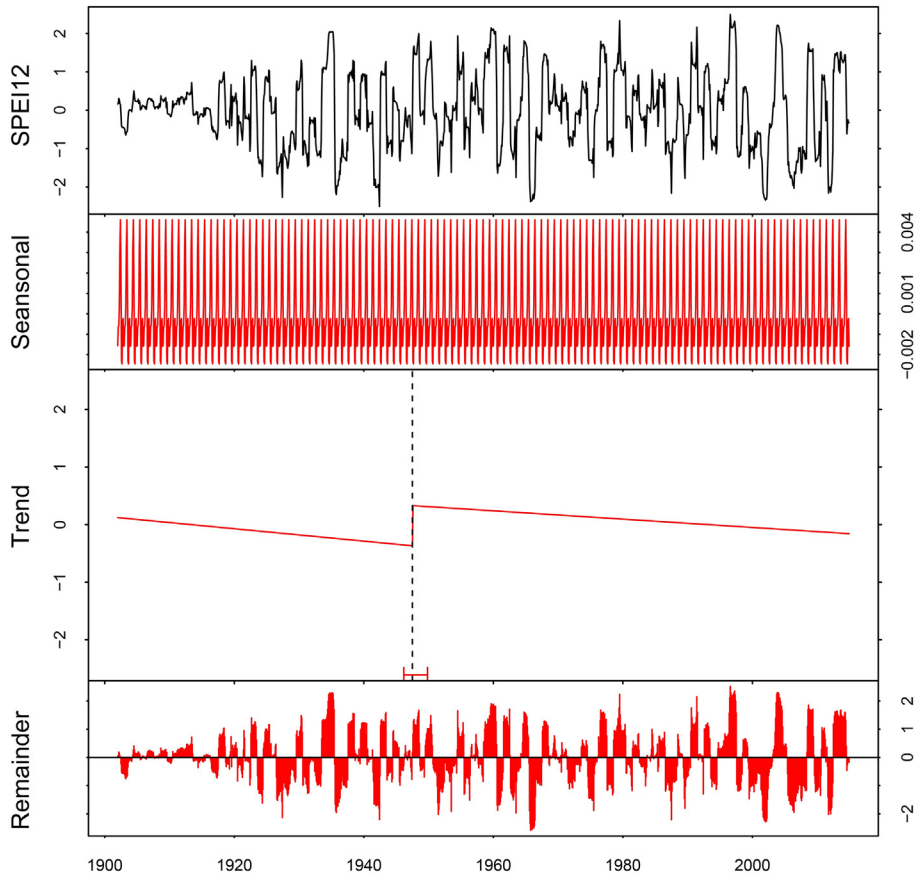

Fig. 3. The BFAST results of regional SPEI12 during 1901–2014 in Inner Mongolia.

later on. The second largest variation type of grids with opposite trend was decrease-increase-increase (D-I-I) type, with 43 grids in total. They were mainly distributed in the central and western regions that belonged to the arid zone. Other variation types accounted for a smaller proportion and were mainly observed in the southwestern and northeastern regions. Due to influence and disturbance from human activities and natural factors, the variation of drought index occurred consequently. Overall, recently, drought index demonstrated a decreasing trend that accounted for 83.7% of the total grids, and there were 284 and 142 grids in the cold semihumid and semiarid zones, respectively (Table S3), indicating a tendency of drought in both semiarid and cold semihumid region.

Fig. 4 showed only the trend variation types of SPEI12 and the number of grids. The amplitude of trend before and after breakpoint and its significance were not described yet. Thus, we drew Fig. 5, trends of SPEI12 before and after breakpoint, based on the calculation results derived from BFAST. The results illustrated that there were 269 grids with one breakpoint, which were mainly distributed in the cold semihumid and semiarid zones, accounting for 49.07% and 44.98% of the total breakpoints, respectively. 196 girds of drought index displayed a decreasing trend before breakpoint, among which 185 grids above the 95% confidence level, suggesting that most grids had an obvious dry tendency before breakpoint. Among 73 grids of drought index with increased trend, 66 grids were above the 95% confidence level (Fig. 5a). After breakpoint, 208 grids of drought index displayed a decreasing trend, among which 204 grids were above the 95% confidence level. Only 32 grids of drought index showed a significant increasing trend after breakpoint, accounting for approximately 52.5% of the increased grids (Fig. 5b). Overall, 218 grids had a significant variation trend before and after breakpoints, among which 83.9% of the grids had a decreasing trend both before and after breakpoints, and 5 grids of drought index first showed an increase and then an increasing trend in the cold semihumid zone. The rest of the grids displayed an increasing trend both before and after breakpoints. The amplitude of trend peaked in the central region, and decreased gradually towards the northeast and southwest directions.

There were 355 grids with two breakpoints in Inner Mongolia, mainly distributed in the northeastern and southwestern regions, which belonged to the arid and cold semihumid zones, respectively, the corresponding proportion was 41.41% and 47.89% in total two breakpoints grids, and only 10.70% grids were sparsely distributed in the semiarid region. In the first time interval, 246 grids of trend were above the 95% confidence level, among which 105 grids of drought index had a decreasing trend and were mainly distributed in the southwestern region and the central and northern region. The other 141 grids had a significantly increasing drought index, and were mainly distributed in the western region and the northeastern region. The amplitude, however, was relatively small, ranging from 0.00546 to 0.39945/10a (Fig. 5c). In the second time interval, 321 grids showed a significantly changing trend, the ones with a decreasing drought index were distributed mainly in the northeastern region and the ones with an increasing drought index were mainly in the southwestern region. It suggested an obvious difference, one region with a significant gain of drought occurrence and the other region with a significant loss of drought occurrence (Fig. 5d). In the third time interval, the spatial distribution pattern was similar to that in second time interval (Fig. 5e). The difference, however, existed between spatial distributions of the high amplitude of trend of drought. For instance, in the third interval, the high value was biased towards the central and eastern region while that was peaked in the edges of southwestern and northeastern. It suggested that in the northeastern and southwestern regions, drought pattern shifted in a relatively frequent manner.

The histogram in Fig. 5 demonstrates the number of breakpoint times of drought index. The left blue bars mean the time distribution

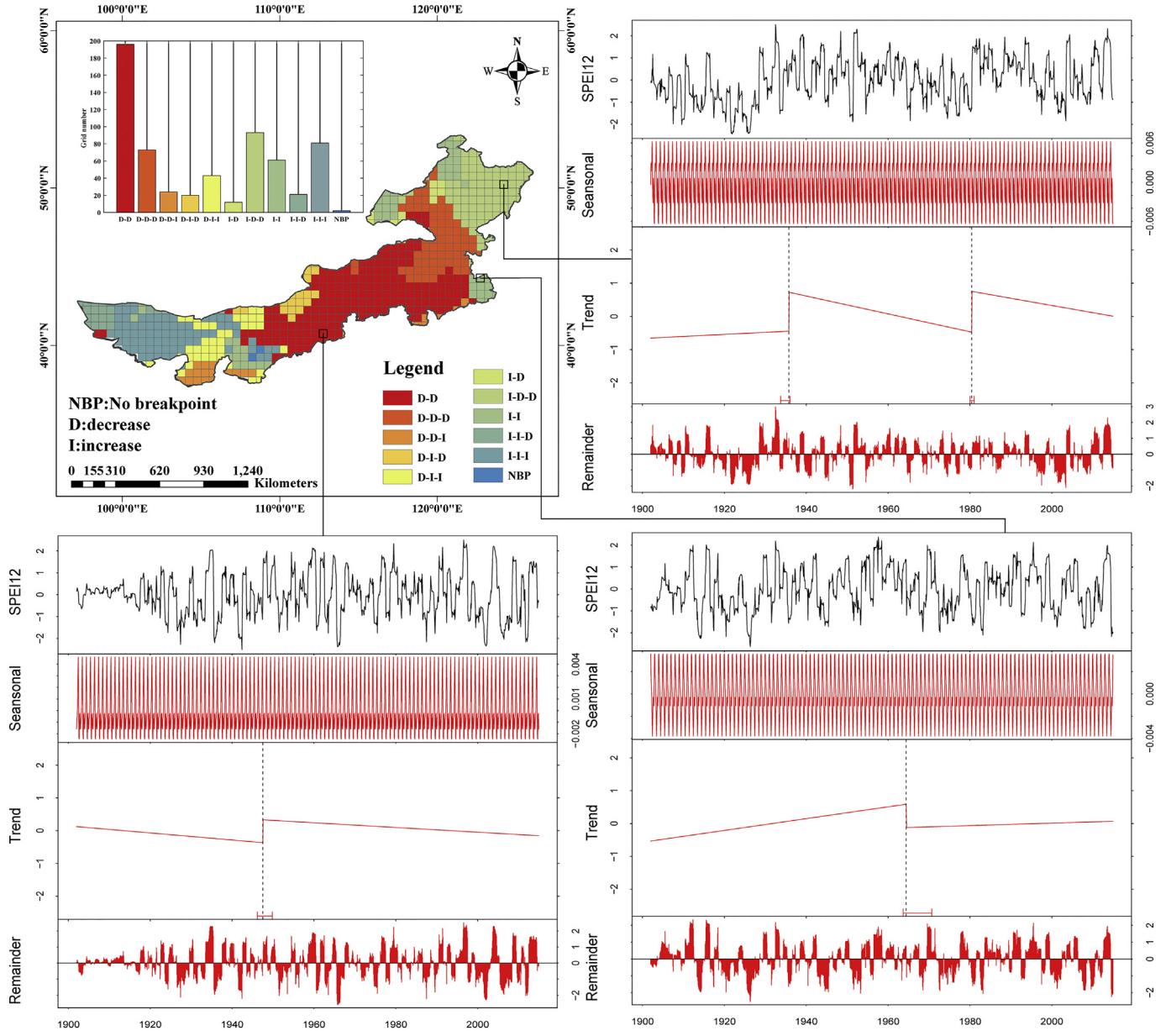

Fig. 4. Variation types of trend of SPEI12 in space.

of first breakpoint times during 1901–2014, and the right rosy bars depict the year corresponding to the second breakpoint. The first breakpoints were mainly in the interval of 1934–1946. From the middle 1930s to the early 1940s, the number of grids of breakpoint in each year was relatively stable; breakpoints of drought index occurred each decade during this period, suggesting that this time interval was a continuous drought sensitive period, subject to external disturbance. However, the second breakpoints were distributed sparsely in 1974–1980. In 1979, there were 205 grids of breakpoints.

As the previous analysis suggested, the year 1979 witnessed an important breakpoint of drought in Inner Mongolia; in the meantime, China entered a rapid development era because of the reform and opening up policy. Therefore, we chose two periods to calculate the trend of annual SPEI and compared the differences between 1901–1979 and 1980–2014 (Fig. S1). Only 63 grids showed a decreasing trend over time and were mainly located in the semiarid and arid zones, the minimum amplitude was -3.960×10^{-3}/a, and 89.94% grids tended to be wetter than before. However, this proportion was reduced to 35.46% during 1980–2014. Both the increased-grids of annual SPEI and the rate of change increased, the minimum amplitude of which was up to −0.0488/a. 326 grids changed from wetting to drying after 1979, and the eastern region mainly presented a trend of drought and the western region a trend of wet. To sum up, though segment-specific trend and overall trend had internal correlation, they might differ in temporal and spatial distribution patterns. If only overall linear trend was analyzed, it might neglect the characteristics of variation of drought in long-term time series. The presence of breakpoints suggested that regarding drought index, the entire series was not homogeneous any more. The potential factors that had driven drought changed greatly. Therefore, it is particularly necessary to assess the non-stationarity characteristics of drought in Inner Mongolia.

3.3. Variation characteristics of drought intensity

In the research, we classified the gridded drought of each decade into five categories, and counted the grid number of transitions from one-time interval to the next time interval for each drought category during 1901–2014. The results indicated that transitions between

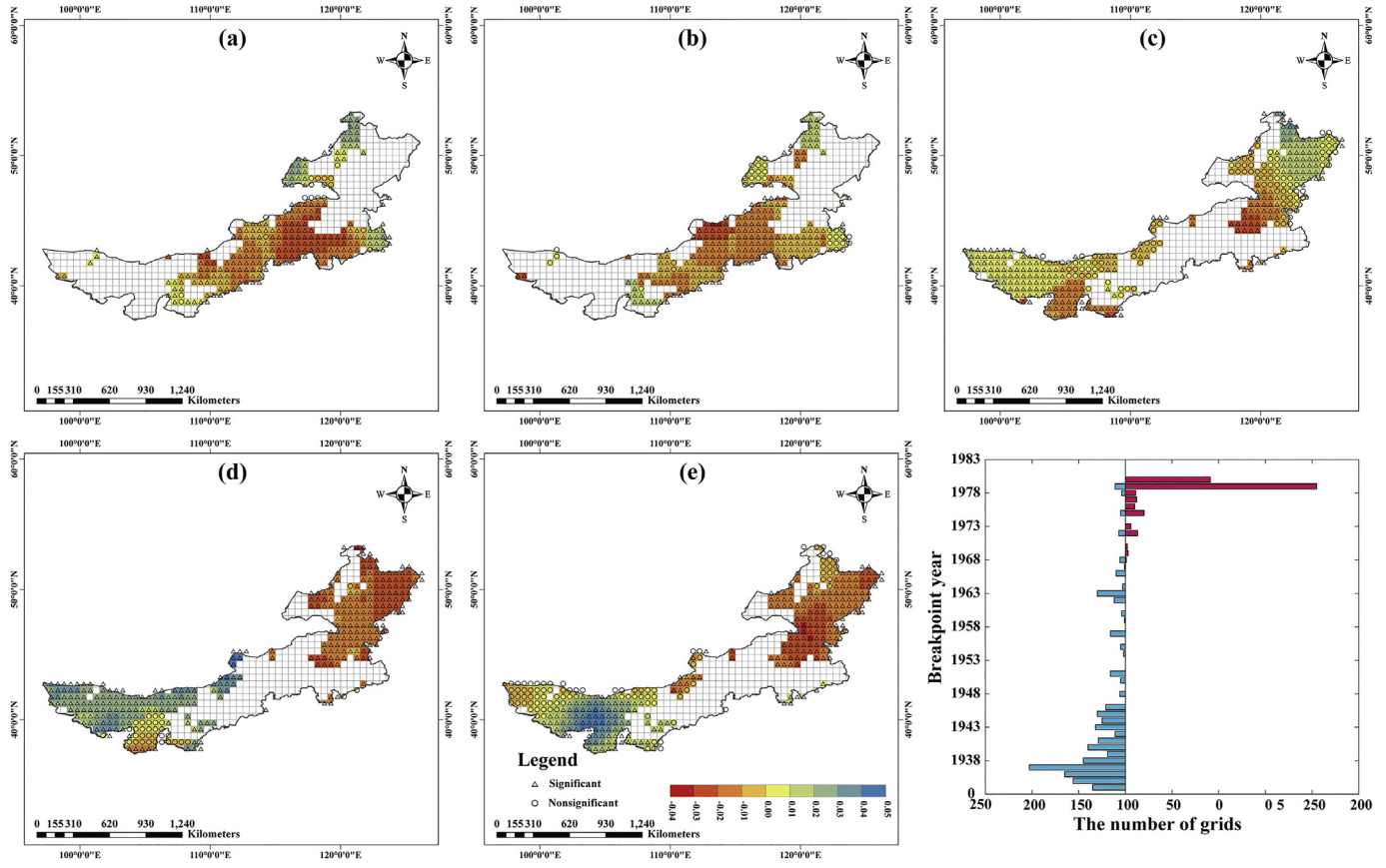

Fig. 5. Spatial distributions of drought change trend before and after breakpoint in Inner Mongolia.

different categories could be observed for each time interval. However, the transition modes were different among time intervals (Fig. S2). Thus, Intensity Analysis method was introduced to quantitatively analyze transition intensity for each time interval, (Fig. S3). The bars that extend to the left of zero stands for change grids of drought in each time interval and the bars that extend to the right of zero was change intensity of drought represented by annual change grids. The solid line means the uniform change intensity of drought during 1901–2014. If an intensity bar ends to the right of the uniform line, it means that the change was relatively fast for that time interval, and if intensity bar ends to the left of the uniform line, it means that the change was relatively slow for that time interval. The change intensity of drought displayed a trend of increasing first and then decreasing. The drought intensity changed the fastest during the interval of 1960–1970, increasing from 38.0% to 88.5% during the interval of 1910–1920, and then gradually decreased to 57.85% during the interval of 2000–2014.

However, what are the mutual transition patterns among categories and the variation trend of categories in each time interval? Fig. 6 well depicts whether the rate of change is dormant versus active for different categories in each time interval. Each category has a pair of horizontal bars. The above bars show the gross losses of the number of grids of drought category and drought intensity of interest; the below bars show the gross gains of the number of grids of drought category and drought intensity of interest. The bars that extend to the right of zero show annual gain or annual loss of variation intensity in each category within an interval; and the bars that extends to the left of zero show annual gain or loss of number of grids in each category within an interval. The vertical solid line represents the uniform line of annual variation intensity within an interval. If an intensity bar ends to the right of the solid line, then the change was relatively active for the corresponding category for that interval; if an intensity bar ends to the left of the solid line, then the change was relatively dormant for the corresponding category for that interval. According to the uniform line of annual variation intensity, the change in the interval of 1960–1970 was relatively active, with an average intensity being 8.85%; except for mild drought, variation intensity for all other drought categories were relatively active, which verified the correctness of results in Fig. S3. Specifically, though transitions of mild, moderate, and severe drought categories during the interval of 1910–1920 were relatively active, their amplitude of change area and intensities of change were close to each other, suggesting many mutual transitions among the three categories. No drought changed a little, and extreme drought witnessed a large increase, which surpassed the uniform line; it suggested that most other categories transitioned to extreme drought (Fig. 6a). The changing situation in the interval of 1920–1930 was similar to the previous interval. However, the uniform value of annual variation intensity during this interval reached 4.15%, and the change of mild, moderate, and severe drought categories were relatively active (Fig. 6b). In the interval of 1930–1940, loss intensity of extreme drought, gain intensities of mild and moderate drought were relatively active, which indicates that the drought severity in the study area has been weakened (Fig. 6c). In the interval of 1940–1950, annual variation intensity continued to increase, and the uniform value of annual variation intensity increased to 7.24%. Change of mild drought was relatively dormant. The amplitudes of gain intensities were larger than that of loss in drought categories of moderate, severe and extreme (Fig. 6d). In the interval of 1950–1960, compared with other categories, variation intensity of no drought was relatively dormant, but the area of no drought has increased. The loss intensities of moderate and severe drought were relatively active (Fig. 6e).

In the interval of 1960–1970, the variation intensity of transitions peaked, with uniform annual variation intensity reaching 8.85%. In this time interval, gain intensities of drought with higher severity were relatively active, with variation intensity of extreme and severe drought

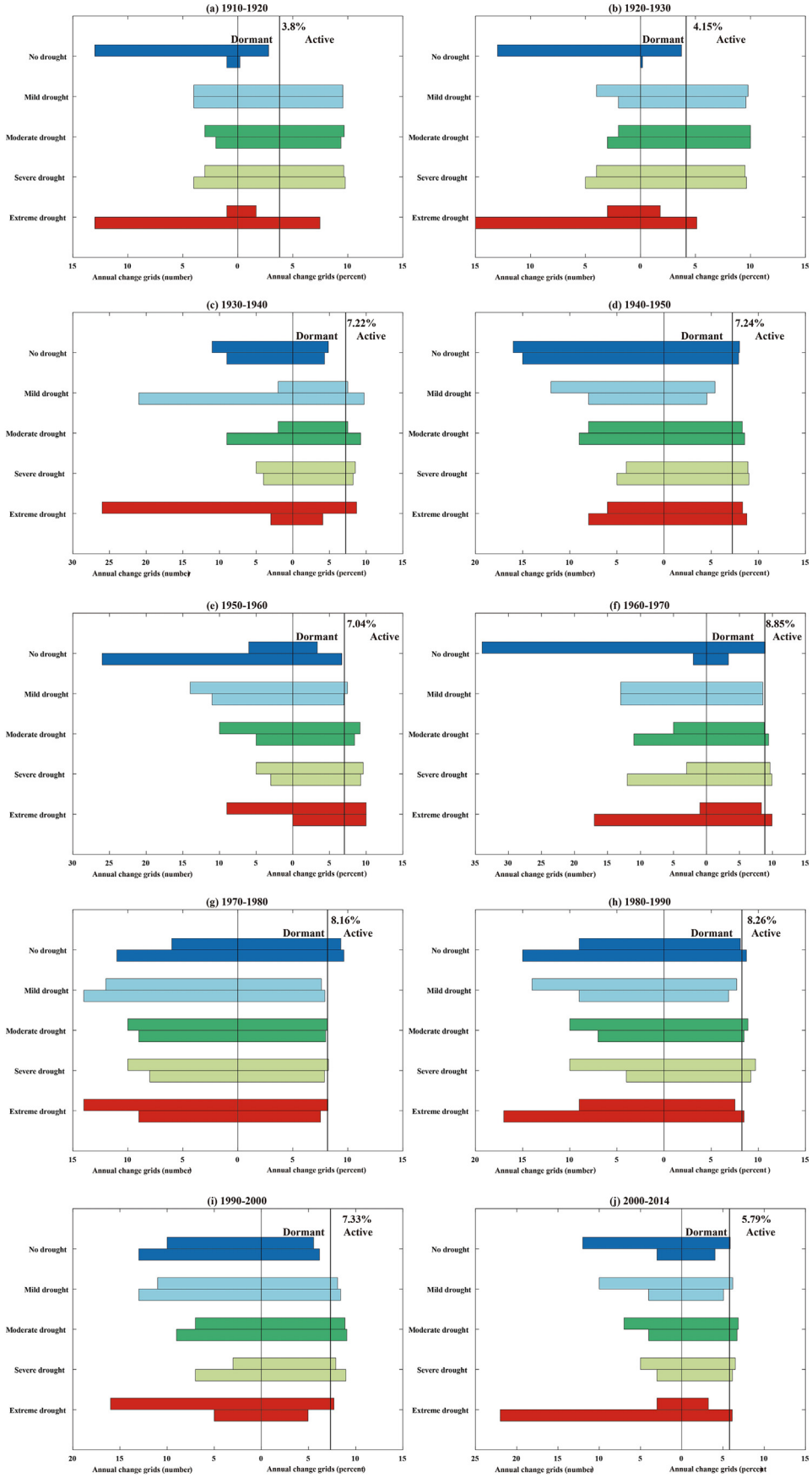

Fig. 6. Intensity analysis of change for each category in Inner Mongolia.

being 9.94% and 9.92%, respectively (Fig. 6f). In the interval of 1970–1980, variation intensity of transitions between categories slowed down, uniform value of variation intensity decreased to 8.16%, with the gain and loss of variation intensity of no drought beyond the uniform line, suggesting that in this time interval, the transitions were mainly from other categories to no drought (Fig. 6g). In the interval of 1980–1990, variation intensity of transitions was second to that in the interval of 1960–1970, with its uniform annual variation intensity being 8.26%. In this time interval, gain and loss of variation intensities of mild drought and losses of variation intensities of no drought and extreme drought were relatively dormant, and that of other categories was relatively active, with loss of variation intensity of severe drought being most active and its value being 9.70% (Fig. 6h). In the interval of 1990–2000, the change of drought intensity is similar to that of 1930–1940, among which the changes of mild, moderate, and severe drought were relatively active. Besides, loss of variation intensity of extreme drought was relatively active (Fig. 6i). In the interval of 2000–2014, uniform variation intensity continued to decrease until 5.79%, among which loss of variation intensities of mild, moderate and severe drought and gain of variation intensity of extreme drought were relatively active (Fig. 6j). To sum up, based on the intensity analysis at category level, we can see that the transition forms changed from being relatively dormant in the interval of 1920–1930 to being relatively active in the interval of 1930–1940, and the trend continued till the interval of 1960–1970. After that, the trend gradually slowed down, suggesting that the climate background experienced a significant change in the intervals of 1930–1940 and of 1960–1970 in the study region. Such results can help detect whether variation intensity of categories in each time interval was relatively active versus dormant. However, what are the mutual transition forms among categories? That requires research at the transition level.

Fig. 7 showed the analysis results at the transition level, which portray the intensity of a category loss to other categories within a time interval. The upper part of the coordinate describes intensity of transition from category i to category n (gain); the lower part describes intensity of transition from category m to category $j(j \neq m)$ (loss). Fig. 7 can reflect which categories have the most dramatic transition to or from other categories within each time interval. The horizontal dashed line in the upper part represents the uniform intensity of transition from any category i to category n and the horizontal dashed line in the lower part represents the uniform intensity of transition from category m to any category $j(j \neq m)$. If the vertical bar extends beyond the dashed line, it means that category dominates the transition. To compare major transitions among categories in each time interval, this paper also presents transitions from and to major drought categories in each time interval (Table S4). The results showed that as for no drought, it mainly transitioned to mild, moderate and severe categories, and the most dramatic losses occurred in the intervals of 1910–1930. In other time intervals, though dramatic transitions existed between no drought and other categories, the change in the number of grids was relatively small due to

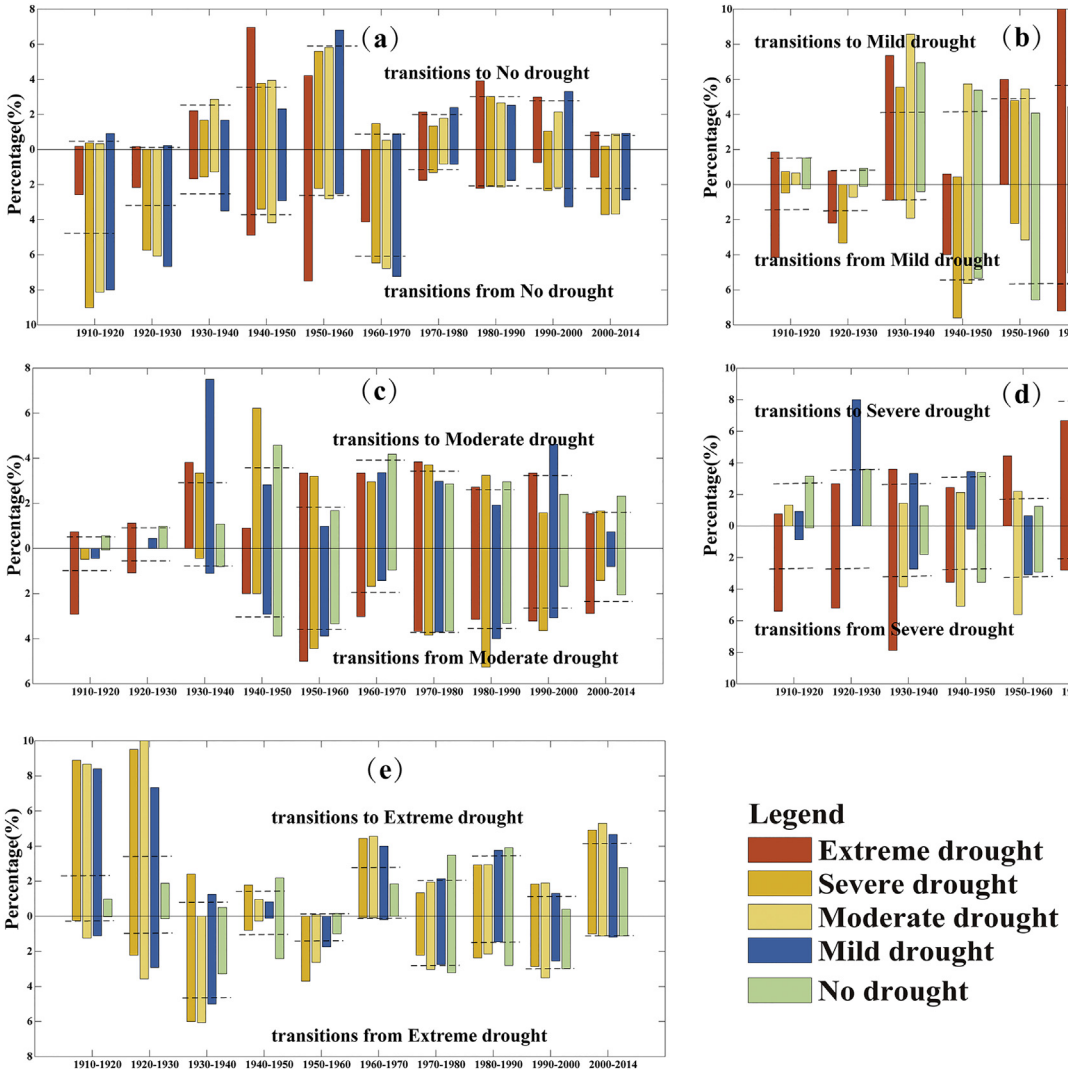

Fig. 7. Intensity analysis of transition among drought categories at each time interval.

their reversible mutual transitions. As for the transition situation of mild drought, it mainly lost to extreme and severe drought, and gained mainly from extreme drought, no drought, and moderate drought, and the most dramatic transitions occurred in the intervals of 1960–1970 and 1990–2000, with the percentage of pixels transitioning from mild drought to extreme drought reaching 10%. Thus, the transition of mild drought was dominated by loss to extreme drought. As for the transition of moderate drought, it lost mainly to severe and extreme drought, and gained mainly from no drought. The gains of severe drought were mainly from no drought, mild and moderate drought during 1920–1930, 1970–1980 and 1990–2000 while that of losses mainly transition to extreme drought during earlier decades.

3.4. Gathering characteristics of drought

To study temporal and spatial interannual variation patterns of drought in Inner Mongolia, we introduced EOF analysis method into this research, and conducted EOF analysis of SPEI12 in Inner Mongolia. The results showed that the first eight eigenvalues of the eigenvector field contributed to 81.07% of the total variance (Table S5), which reflected the characteristics of variate field of drought index and spatial anomaly. By analyzing the distribution of eigenvalue modes of EOF eigenvector field, the results illustrated that the first and second explained variance differed greatly with other variances in contribution to variance. As the number of modes increased, its contribution to variance gradually diminished, and the rate of diminishing (decelerating rate) gradually reduced. It suggested that vast territory and various geographical conditions and climate states between the east and the west of the study region led to significant regional differences in drought features across Inner Mongolia.

Testing method proposed by North et al. (1982) was adopted to conduct significance testing towards eigenvalues, and percentages of explained variance for each EOF of the SPEI12 were provided in the Supplementary materials (Table S5). The results showed that the first two modes were above the 95% confidence level, suggesting that the eigenvector included meaningful information on drought characteristics. The first two modes were the most important two spatial abnormal modes, which could reflect the spatial distribution pattern of rate of drought changes.

The spatial distribution of EOF mode1 (Fig. 8a) showed that the variation intensity of drought had similar oscillation phases and the direction of variation trend in Inner Mongolia. It suggested that the entire Inner Mongolia had been influenced and controlled by weather system under the uniform scale, thus leading to tendency to consistent spatial distribution of drought index. Another feature was that the absolute value of eigenvector gradually decreased from the central region towards the northeast and southwest directions. The areas with negative absolute value of eigenvector ≥ 0.2557 occurred in the central region of Inner Mongolia, which suggested that the amplitude of variation of drought index was the largest in this area, which was the most sensitive and likely to witness drought anomaly. If the component values of the eigenvector field are <0, the time coefficient of the eigenvector field of the drought index is larger than 0, indicating that the whole region shows a consistent drought phenomenon. The higher the value is, the more typical the distribution pattern of drought of the year would be. When time coefficient is less than zero, it means that it was a year of no drought; the higher the value is, the more typical the distribution pattern of no drought of the year would be. The years of consistent drought were mainly in the intervals of 1910–1930 and 1999–2010; the years of consistent no drought were mainly in the intervals of 1943–1963 and 1985–1999. Climate tendency rate of corresponding time coefficient of eigenvector field in EOF mode1 was 2×10^{-5}/decade ($R^2 = 0.0007$), and the time coefficient showed an increasing trend, but did not reach the 95% confidence level, suggesting that the variation intensity of drought was fluctuant and has stationarity characteristics in the entire region.

Eigenvector field of EOF mode2 reflected the anti-phase characteristics of drought in the eastern and western regions in Inner Mongolia (Fig. 8b). The demarcation line of component value of eigenvector field equal to zero divided the study region into two parts: the eastern region and the western region. Each eigenvector value in the western region exceeded zero, accounting for 50.07% of the total number of grids. The maximum value of eigenvector component occurred in the central of the western region (131 grids), with its rate of change ranging from 0.1683 to 0.2521. Each eigenvector value in the eastern region less than zero, the center of largest negative absolute value of eigenvector component occurred at the farthest northeastern border. It suggested that this region had the largest amplitude of drought change, and was the most sensitive area of its differentiation type. The eastern region was influenced not only by temperate continental climate, but also by oceanic climate; the western region, however, was influenced mainly by temperate continental climate. These features led to the anti-phase spatial distribution structural characteristics between the eastern and the western regions. Climate tendency rate of corresponding time coefficient of eigenvector field in EOF mode2 was -2×10^{-4}/decade ($R^2 = 0.074$), and time coefficient showed a decreasing trend, which reflected

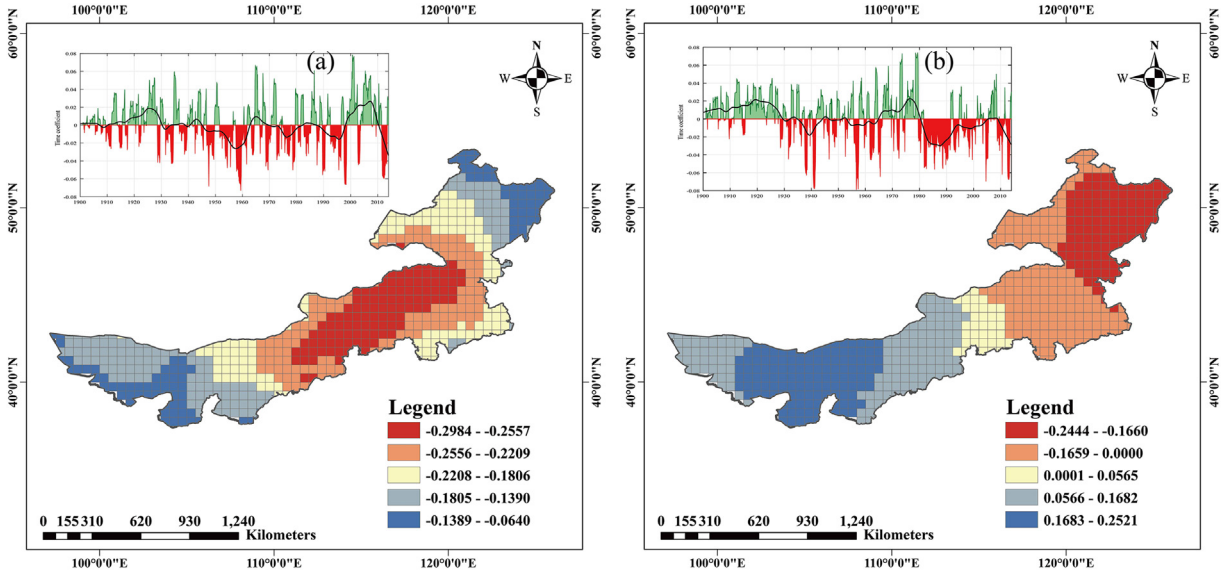

Fig. 8. Spatial distribution of two leading modes of SPEI12 for EOF eigenvectors.

major characteristics, such as a tendency for intensity of drought to decrease in the western region and eastern regions displayed an opposite trend. The eastern region followed the consistent pattern of drought 1940–1980 while the western regions followed the consistent pattern of no drought during 1980–2000.

4. Discussion

In the past one hundred years, intensification of global warming and human activities has severely undermined the global and regional water and heat balance, which further leads to aggregation of drought phenomenon and continuous expanding of arid areas in the future (Huang et al., 2016). As non-stationarity phenomenon of drought has been increasingly prominent, the trend analysis and breakpoints detection become major means to determine whether non-stationarity hypothesis is rational or not. This study employed and BFAST algorithm to investigate the spatiotemporal variation characteristics of drought. We found that the drought index of the study area has not changed linearly in the past one hundred years and one or two breakpoints have been detected in time series. The results suggested that there were many variation types of drought and spatiotemporal variation among time intervals. This phenomenon existed both before and after the breakpoints of drought index in Inner Mongolia, which demonstrated that variation of drought had obvious non-stationarity characteristics. In this research, the results suggested that the central and eastern regions got drying trends, which was similar to the previous research conclusion in the arid regions in Inner Mongolia (Wang et al., 2017). We found that the northeastern region displayed an I-D-D type of trend in drought. Results of Liu et al. (2016b) displayed an I-D type of trend in the corresponding areas. With further analysis, the time scale of the drought index, methods and study period in two studies were different. Greve et al. (2014) pointed out about 10.8% of the global land was strictly consistent with the trend pattern of "the dry gets drier and the wet gets wetter". The D-D and D-D-D, types of drought variation in semiarid zone were consistent with the point.

In order to verify the accuracy of the results of this paper, we calculated the overall linear trend of gridded SPEI12 for whole Inner Mongolia (Fig. S4). We found that SPEI12 in the northeastern part of the study area showed an upward trend, indicating that there was no tendency of drought. However, the trend of drought characterized by observed SPEI (calculated based on monthly precipitation and monthly average temperature of weather station data) illustrated that there was an increasing trend of drought in the corresponding area, which was consistent with the findings of our study. Climate change is a long-term and fluctuating process. It is possible that it displays an increasing or decreasing trend within a short interval, which might become just a slight oscillation in a longer time series. Therefore, it is necessary to explore stationarity characteristics in the study of climate change in long-term scale. Additionally, compared with the change of drought characterized by area (Li et al., 2014; Tong et al., 2018), the study uses the drought intensity, which can comprehensively express the drought within a time interval and better applicability in the intensity analysis method. The application of the EOF method has played a very good auxiliary role, and the results have objectively confirmed the temporal and spatial variation characteristics of drought in Inner Mongolia again. We used long-term time series to explore the temporal and spatial characteristics of drought change, which could enrich drought research in Inner Mongolia and provide a scientific as well as a practical reference for effective prevention of drought disasters.

Inner Mongolia, located to the south of Mongolian Plateau, in recent decades, has witnessed the expanding of desert area due to overgrazing and rapid urbanization etc. (Song et al., 2017). Such land use changes have led to significant climate change in the study region, which might contribute to the occurrence of drought. To discuss the natural environment of the study area, we used nine meteorological factors extracted from TerraClimate dataset to calculate Pearson correlation coefficient with annual SPEI to explore the potential relationships between them (Figs. S5 and S6). The results illustrated that for the nine meteorological factors, AET and SM were the most sensitive factors affecting drought intensity in Inner Mongolia, 81.95% and 73.16% grids of which showed a positive correlation with SPEI, and the number of grids above the 95% confidence level accounted for 42.17% and 15.81%, respectively. Mainly located in the middle of the study area, and the western region of the arid zone. The above areas were also the drought prone areas in Inner Mongolia. The greater the SM and AET are, the smaller the intensity of meteorological drought will be. DEF is the difference between ET0 and actual evapotranspiration, 40.73% grids demonstrated a significant negative correlation with SPEI, which were mainly located in the intermediate region. The distribution of PET also followed this spatial pattern. Latent heat amplified the most extreme events by the largest amount, and changes in atmospheric circulation drove larger increases in more extreme precipitation events compared with less extreme ones (Pendergrass, 2018). Therefore, the higher of SRAD, TMAX and TMIN, the drier will be in most of the region, especially in the middle region; the effects of the lowest temperature were relatively small compared with the other two meteorological factors. However, the region was far from the sea, the correlation between WS and SPEI was not so significant, with only 4.45% grids above the 95% confidence level.

Using SPEIbase v2.4 from The Global 0.5°gridded SPEI dataset, we conducted investigation on drought characteristics in Inner Mongolia during 1901–2014. Despite the achievements, this study was still faced with limitations. Firstly, Fischer and Knutti (2015) pointed out that arid region of Inner Mongolia also got drier. However, about 9.5% of the terrestrial area showed a trend pattern of "the dry gets wetter and the wet gets drier" in Inner Mongolia. This dataset was calculated based on CRU temperature and precipitation dataset. The intrinsic variation of simulation of meteorological factors would undermine the precision to depict temporal and spatial distribution of drought index. Therefore, comparison validation with different datasets seems to be of particular necessity. Besides, the causes for the formation of drought can be complicated, and different causing factors might aggregate or mitigate each other's effects, or just trade off and take turns to play their roles. So how to define the internal correlation between natural and manufactured factors and rate of their contribution to the occurrence of drought events has not been addressed in this paper. For instance, frequent occurrence of El Nino phenomenon might exert an impact on terrestrial hydrological cycle, which further influences the formation of drought. All these issues should be dealt with in future studies.

5. Conclusion

In this paper, the temporal and spatial variation of non-stationarity characteristics of drought, the transition intensities among drought categories and gathering characteristics of drought was analyzed during 1901–2014 in Inner Mongolia by using BFAST, intensity analysis and EOF methods, respectively. Conclusions are as follows:

(1) Non-stationarity characteristics. The research suggested a decreasing trend of regional drought over the entire region, detected a breakpoint in drought in 1945. The amplitude in drought trends after breakpoints was −0.007/a and above the 95% confidence level. There were 196 grids of decrease-decrease type, 73 grids of decrease-decrease-decrease type and 93 grids of increase-decrease-decrease variation types of SPEI12, which mainly occurred in the central parts of the semiarid, central and northeastern cold semihumid zone, respectively. The three types of variation indicated that the climate in these areas had a tendency of drought.
(2) Variation intensity. The overall drought intensity displayed an increasing trend first, which was followed by a decreasing trend. The variation intensity increased fastest from 38.02% in

1910–1920 to 88.50% during 1960–1970; then it gradually decreased to 57.85% during 2000–2014. The gain intensity of extreme drought was relatively active in periods of 1960–1970 and the severity of the drought has decreased during the periods of 1930–1940 and 1990–2000, respectively.

(3) Gathering characteristics. EOF mode1 showed that variation intensity of drought with not significantly increased trend in the entire region, the drought with high amplitude was likely to occur in the central regions. EOF mode2 showed that variation intensity of drought displayed the opposite phases between the eastern and the western regions, among which the northeastern regions were the prone areas with high amplitude of drought. The area with high amplitude in EOF mode1 and EOF mode2 were similar to the spatial distribution of D-D-D, D-D and I-D-D, which further verified the results of BFAST.

Supplementary data to this article can be found online at https://doi.org/10.1016/j.scitotenv.2018.10.425.

Acknowledgements

This study was supported by the Science and Technology Innovation Project "Grassland Non-biological Disaster Prevention and Mitigation Team" of Chinese Academy of Agricultural Sciences (CAAS-ASTIP-IGR2015-04), and China Postdoctoral Science Foundation Funded Project (2017M620975).

References

Abatzoglou, J.T., Dobrowski, S.Z., Parks, S.A., Hegewisch, K.C., 2018. TerraClimate, a high-resolution global dataset of monthly climate and climatic water balance from 1958–2015. Sci. Data 5, 170191.

Abramopoulos, F., Rosenzweig, C., Choudhury, B., 1988. Improved ground hydrology calculations for global climate models (GCMs): soil water movement and evapotranspiration. J. Clim. 1, 921–941.

Aldwaik Jr., S.Z., Pontius, R.G., 2012. Intensity analysis to unify measurements of size and stationarity of land changes by interval, category, and transition. Landsc. Urban Plan. 106 (1), 103–114.

Chen, T., Zhang, H., Chen, X., Hagan, D., Wang, G., Gao, Z., Shi, T., 2017. Robust drying and wetting trends found in regions over China based on Köppen climate classifications. J. Geophys. Res.-Atmos. 122 (8), 4228–4237.

Dai, A.G., Trenberth, K.E., Tian, T.T., 2004. A global dataset of Palmer Drought Severity Index for 1870–2002: relationship with soil moisture and effects of surface warming. J. Hydrometeorol. 5 (6), 1117–1130.

Fischer, E.M., Knutti, R., 2015. Anthropogenic contribution to global occurrence of heavy-precipitation and high-temperature extremes. Nat. Clim. Chang. 5 (6), 560.

Greve, P., Orlowsky, B., Mueller, B., Sheffield, J., Reichstein, M., Seneviratne, S.I., 2014. Corrigendum: global assessment of trends in wetting and drying over land. Nat. Geosci. 7 (10), 848.

Grogan, K., Pflugmacher, D., Hostert, P., Verbesselt, J., Fensholt, R., 2016. Mapping clearances in tropical dry forests using breakpoints, trend, and seasonal components from MODIS time series: does forest type matter? Remote Sens. 8 (8), 657.

Guo, E., Liu, X., Zhang, J., Wang, Y., Wang, C., Wang, R., Li, D., 2017. Assessing spatiotemporal variation of drought and its impact on maize yield in Northeast China. J. Hydrol. 553, 231–247.

He, B., Wu, J., Lü, A., Cui, X., Zhou, L., Liu, M., Zhao, L., 2013. Quantitative assessment and spatial characteristic analysis of agricultural drought risk in China. Nat. Hazards 66 (2), 155–166.

Huang, J., Xue, Y., Sun, S., Zhang, J., 2015. Spatial and temporal variability of drought during 1960–2012 in Inner Mongolia, North China. Quat. Int. 355, 134–144.

Huang, J., Yu, H., Guan, X., Wang, G., Guo, R., 2016. Accelerated dryland expansion under climate change. Nat. Clim. Chang. 6 (2), 166–171.

IPCC, 2014. Climate Change 2014: Synthesis Report. Contribution of Working Groups I, II and III to the Fifth Assessment Report of the Intergovernmental Panel on Climate Change (Geneva, Switzerland).

Lambert, J., Denux, J.P., Verbesselt, J., Balent, G., Cheret, V., 2015. Detecting clear-cuts and decreases in forest vitality using MODIS NDVI time series. Remote Sens. 7 (4), 3588–3612.

Li, Z., Zheng, F.L., Liu, W.Z., 2012. Spatiotemporal characteristics of reference evapotranspiration during 1961–2009 and its projected changes during 2011–2099 on the Loess Plateau of China. Agric. For. Meteorol. 154–155 (6), 147–155.

Li, J., Yue, Y.J., Pan, H.M., Ye, X.Y., 2014. Variation rules of meteorological drought in China during 1961–2010 based on SPEI and intensity analysis. J. Catastrophology 29 (4), 176–182 (In Chinese).

Li, F., Song, G., Liujun, Z., Yanan, Z., Di, L., 2017. Urban vegetation phenology analysis using high spatio-temporal NDVI time series. Urban For. Urban Green. 25, 43–57.

Liu, Z., Wang, Y., Shao, M., Jia, X., Li, X., 2016a. Spatiotemporal analysis of multiscalar drought characteristics across the Loess Plateau of China. J. Hydrol. 534 (534), 281–299.

Liu, S., Kang, W., Wang, T., 2016b. Drought variability in Inner Mongolia of northern China during 1960–2013 based on standardized precipitation evapotranspiration index. Environ. Earth Sci. 75 (2), 145.

Liu, M., Xu, X., Xu, C., Sun, A.Y., Wang, K., Scanlon, B.R., Zhang, L., 2017a. A new drought index that considers the joint effects of climate and land surface change. Water Resour. Res. 53 (4), 3262–3278.

Liu, Y., Zhu, Y., Ren, L., Singh, V.P., Yang, X., Yuan, F., 2017b. A multiscalar palmer drought severity index. Geophys. Res. Lett. 44 (13), 6850–6858.

McKee, T.B., Doesken, N.J., Kleist, J., 1993. The Relationship of Drought Frequency and Duration to Time Scales. Proceeding of the Ninth Conference on Applied Climatology. American Meteorological Society, Boston, pp. 179–184.

Mishra, A.K., Singh, V.P., 2010. A review of drought concepts. J. Hydrol. 391 (1), 202–216.

"NARCC"EC, 2015. National assessment report of climate change (III). Science Press, Beijing.

North, G.R., Bell, T.L., Cahalan, R.F., Moeng, F.J., 1982. Sampling errors in the estimation of empirical orthogonal functions. Mon. Weather Rev. 110 (7), 699–706.

Palmer, W.C., 1965. Meteorological droughts. US Department of Commerce Weather Bureau Research Paper. 45, p. 58.

Pendergrass, A.G., 2018. What precipitation is extreme? Science 360 (6393), 1072.

Sheffield, J., Wood, E.F., 2008. Projected changes in drought occurrence under future global warming from multi-model, multi-scenario, IPCC AR4 simulations. Clim. Dyn. 31 (1), 79–105.

Song, Y., Guo, Z., Lu, Y., Yan, D., Liao, Z., Liu, H., Cui, Y., 2017. Pixel-level spatiotemporal analyses of vegetation fractional coverage variation and its influential factors in a desert steppe: a case study in Inner Mongolia, China. Water 9 (7), 478.

Thornthwaite, C.W., 1948. An approach toward a rational classification of climate. Geogr. Rev. 38, 55–94.

Tian, F., Fensholt, R., Verbesselt, J., Grogan, K., Horion, S., Wang, Y., 2015. Evaluating temporal consistency of long-term global NDVI datasets for trend analysis. Remote Sens. Environ. 163, 326–340.

Tong, S., Lai, Q., Zhang, J., Bao, Y., Lusi, A., Ma, Q., Li, X., Zhang, F., 2018. Spatiotemporal drought variability on the Mongolian Plateau from 1980–2014 based on the SPEI-PM, intensity analysis and Hurst exponent. Sci. Total Environ. 615, 1557–1565.

Verbesselt, J., Hyndman, R., Newnham, G., Culvenor, D., 2010a. Detecting trend and seasonal changes in satellite image time series. Remote Sens. Environ. 114 (1), 106–115.

Verbesselt, J., Hyndman, R., Zeileis, A., Culvenor, D., 2010b. Phenological change detection while accounting for abrupt and gradual trends in satellite image time series. Remote Sens. Environ. 114 (12), 2970–2980.

Verbesselt, J., Zeileis, A., Herold, M., 2012. Near real-time disturbance detection using satellite image time series. Remote Sens. Environ. 123 (123), 98–108.

Vicenteserrano, S.M., Beguería, S., López moreno, J.I., 2010. A multiscalar drought index sensitive to global warming: the standardized precipitation evapotranspiration index. J. Clim. 23 (7), 1696–1718.

Wang, Q., Wu, J., Lei, T., He, B., Wu, Z., Liu, M., Mo, X., Geng, G., Li, X., Zhou, H., Liu, D., 2014. Temporal-spatial characteristics of severe drought events and their impact on agriculture on a global scale. Quat. Int. 349, 10–21.

Wang, L., Xing, Y., Xie, Z., Wu, P., Li, Y., 2016a. Increasing flash droughts over china during the recent global warming hiatus. Sci Rep. 6, 30571.

Wang, Y., Zhang, J., Guo, E., Dong, Z., Quan, L., 2016b. Estimation of variability characteristics of regional drought during 1964–2013 in Horqin Sandy Land, China. Water 8 (11), 543.

Wang, Z., Li, J., Lai, C., Zeng, Z., Zhong, R., Chen, X., Zhou, X., Wang, M., 2017. Does drought in China show a significant decreasing trend from 1961 to 2009? Remote Sens. Environ. 579, 314–324.

Wang, H., He, B., Zhang, Y., Huang, L., Chen, Z., Liu, J., 2018. Response of ecosystem productivity to dry/wet conditions indicated by different drought indices. Sci. Total Environ. 612, 347–357.

Wu, H., Hayes, M.J., Wilhite, D.A., Svoboda, M.D., 2005. The effect of the length of record on the standardized precipitation index calculation. Int. J. Climatol. 25 (4), 505–520.

Zhang, Q., Zhang, J., Wang, C., 2017. Risk assessment of drought disaster in typical area of corn cultivation in China. Theor. Appl. Climatol. 128 (3–4), 533–540.

Zhou, Y., Li, N., Ji, Z., Gu, X., Fan, B., 2013. Temporal and spatial patterns of droughts based on Standard Precipitation Index (SPI) in Inner Mongolia during 1981–2010. Chin. J. Nat. Resour. 28 (10), 1694–1706 (In Chinese).